



Polynomial state of the electromagnetic field: generation and statistical properties

Simone Souza ^a, A.T. Avelar ^{*,b}, N.G. de Almeida ^{a,c}, B. Baseia ^{a,*}

^a Instituto de Física, Universidade Federal de Goiás, 74.001-970, Goiânia, GO, Brazil

^b Instituto de Física, Universidade de Brasília, 70.919-970 Brasília, DF, Brazil

^c Núcleo de Pesquisas em Física, Universidade Católica de Goiás, 74.605-220, Goiânia, GO, Brazil

Received 4 December 2003; received in revised form 12 May 2004; accepted 20 May 2004

Abstract

In a previous paper a distinct proposal for measuring the variance of quadrature operators [Phys. Lett. A 238 (1998) 223], based on the projection synthesis method [Phys. Rev. Lett. 76 (1996) 4148], was presented. The scheme requires the use of an unavailable state, named polynomial state (PS). In this report, we discuss the generation of this state in travelling waves, appropriate for the method, and consider its statistical features.

© 2004 Elsevier B.V. All rights reserved.

PACS: 42.50.Dv

Keywords: Quantum state engineering; Projection synthesis method; Polynomial state

1. Introduction

An important issue of quantum optics in the last years concerns the quantum state engineering (QSE), both for field [1–8] and atomic states [9,10]. Its relevance comes from potential applications on advanced topics, as teleportation [11],

quantum computation [12], quantum communication [13], quantum cryptography [14], quantum lithography [15], decoherence of states [16], etc. The field state being tailored may refer to either stationary modes trapped inside a high- Q cavity [1,2] or travelling modes [3–8]. In the first case QSE can be implemented either via resonant [1] or via nonresonant (dispersive) atom-field interaction [2]. In the second case QSE may employ: (i) a coherent state travelling throughout a nonlinear medium [17]; (ii) an array of beam-splitters [3–5],

* Corresponding authors. Tel./fax: +55625211014.

E-mail addresses: ardiley@unb.br (A.T. Avelar), basilio@fis.ufg.br (B. Baseia).

(iii) a Mach–Zehnder interferometer including a nonlinear medium [6], etc.

In a previous paper, Barnett and Pegg [18] showed that an apparent *exotic* state, then named reciprocal binomial state (RBS), not available in laboratories, was crucial for their proposed experimental scheme determining the phase distribution $P(\theta)$ describing an arbitrary state of a running-field. Later on [19], it was shown that the projection synthesis method proposed in [18] can also be used to determine the Husimi Q -function of a field state and the variances of quadratures operators. In these cases, construction of other unknown states, respectively named complementary coherent state (CCS) and polynomial state (PS), were crucial for such determinations. The generations of the RBS and CCS have been addressed in [20,21] for fields in travelling modes, as required in [18]. Here we will consider the generation of PS for fields in travelling modes, suitable for the projection synthesis method. Beyond its potential use for measuring variance of quadrature operators [19] the generation of this *exotic* state may provide us new insights – one example being its use to construct relevant superpositions, such as $c_1|n_1\rangle + c_2|n_2\rangle$ [22].

This report is organized as follows: in Section 2 we introduce the PS and propose its generation through a scheme developed in [5]. The fidelity of the generation process is calculated through the Langevin method. For completeness, Section 3 contains a resumed study about some statistical properties exhibited by the PS. Section 4 contains the comments and conclusion.

2. Generation of PS

The PS was defined previously as [19],

$$|PS\rangle = \mathcal{N} \sum_{n=0}^N \binom{N}{n}^{-1/2} \frac{H_{N-n}(x/\sqrt{2}) e^{i\frac{\pi n^2}{2}}}{\sqrt{(2N-2n-1)!!}} |n\rangle, \tag{1}$$

where x is a parameter of the (auxiliary) PS that selects the value of quadrature operator \hat{x} of the arbitrary state being measured. \mathcal{N} is the normalization constant

$$\mathcal{N} = \left[\sum_{k=0}^N \binom{N}{k}^{-1} \frac{H_{N-k}^2(x/\sqrt{2})}{(2(N-k)-1)!!} \right]^{-1/2}. \tag{2}$$

As the PS is a truncated state, we may employ the scheme introduced in [5]. For completeness, we present a brief summary showing the relevant steps of this procedure. In this scheme a desired state $|\Psi\rangle$ composed of a finite number of Fock states $|n\rangle$ can be written as

$$\begin{aligned} |\Psi\rangle &= \sum_{n=0}^N C_n |n\rangle = \frac{C_N}{\sqrt{N!}} \prod_{n=1}^N (\hat{a}^\dagger - \beta_n^*) |0\rangle \\ &= \frac{C_N}{\sqrt{N!}} \prod_{k=1}^N \hat{D}(\beta_k) \hat{a}^\dagger \hat{D}^\dagger(\beta_k) |0\rangle, \end{aligned} \tag{3}$$

where $\hat{D}(\beta_n)$ stands for the displacement operator and the β_n are the roots of the polynomial equation

$$\sum_{n=0}^N \frac{C_n}{\sqrt{n!}} (\beta^*)^n = 0. \tag{4}$$

According to the experimental setup shown in the Fig. 1 we have that the outcome state is (assuming zero-photon registered in all detectors),

$$|\Psi\rangle \sim \prod_{k=1}^N \hat{D}(\alpha_{k+1}) \hat{a}^\dagger T^{\hat{n}} \hat{D}^\dagger(\alpha_k) |0\rangle, \tag{5}$$

where T is the transmittance of the beam splitter and α_k are experimental parameters. After some algebra Eqs. (3) and (5) can be connected. These equations become identical when $\alpha_1 = -\sum_{l=1}^N T^{-l} \alpha_{l+1}$ and $\alpha_k = T^{*N-k+1} (\beta_{k-1} - \beta_k)$ for $k=2,3,4,\dots,N$. In the present case the coefficients C_n are given by those of the PS, hence the roots β_k^* of the characteristic polynomial in Eq. (4) are calculated and the displacement parameters α_k^* can be obtained for specific values.

The success probability \mathcal{P} of producing the PS is shown in Fig. 2, for $N=5$. In this figure, for each small x -interval, we have used the transmittance of the beam-splitters in a way to optimize the success probability. Since the ideal procedure would use the appropriate transmittance for each value of x , this approximation avoiding lengthy

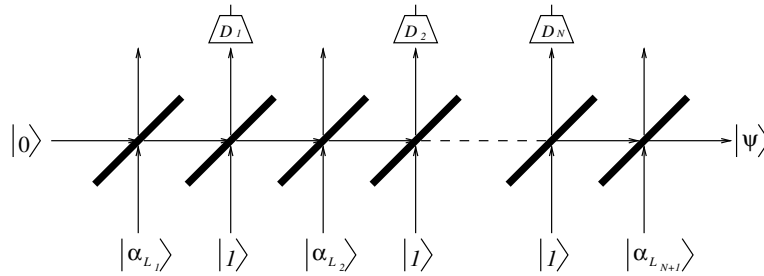


Fig. 1. Experimental setup of the BSA scheme (cf. [5]).

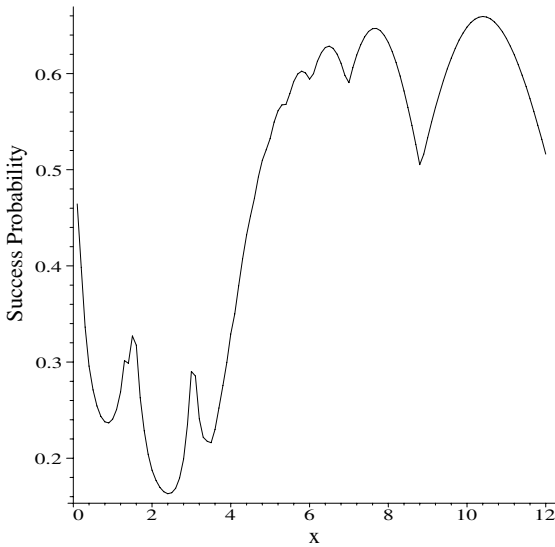


Fig. 2. Plot of success probability (%) versus x .

computer calculation, causes the oscillations in the success probability shown in Fig. 2. It is assumed that the beam splitters used for photon adding have the same transmittance. We note in Fig. 2 that the success probability is about $\mathcal{P} \simeq 0.5\%$. Similar plots for $N=3$ and $N=7$ show that $\mathcal{P} \simeq 5\%$ and $\mathcal{P} \simeq 0.05\%$, respectively (not shown in figures). So, the probability decreases for growing N , as expected.

Till now we have assumed all detectors and beam-splitters as ideal. While excellent beam-splitters are available in laboratories by the advanced technology, the same is not true for photodetectors in the optical domain, although recent

progress has been achieved in this direction [23]. So, let us now take into account the quantum efficiency η of the photodetectors. To this end we use the Langevin operator technique, as applied in [8], in order to obtain the fidelity of the PS got from the scheme of [5].

In this scheme the output operator accounting for the detection of a field \hat{a}_{out} is given by $\hat{a}_{\text{out}} = \sqrt{\eta}\hat{a}_{\text{in}} + \hat{L}_a$, where η stands for the efficiency of the detector and \hat{L}_a , acting on environment states, is the noise or Langevin operator associated with losses in the detector registering photons in the mode a . We assume that the detector couple neither different modes a, b nor environment modes (associated to the Langevin operators \hat{L}_a), so the following commutation relation is readily obtained: $[\hat{L}_a, \hat{L}_a^\dagger] = 1 - \eta$.

The ground-state expectation values for Langevin operator is $\langle \hat{L}_a \hat{L}_a^\dagger \rangle = 1 - \eta$, which is useful relation mainly for optical frequencies, when the state of the environment can be very well approximated by the vacuum state, even for room temperature: $KT_{\text{env}} \approx (1/40)$ eV and $h\nu_{\text{opt}} \approx 1$ eV; hence $h\nu_{\text{opt}}/KT_{\text{env}} \approx 40$ and we find that $\langle n_{\text{env}} \rangle = 1/[\exp(h\nu_{\text{opt}}/KT_{\text{env}}) - 1] \approx 0$.

Let us now apply the scheme of the [5] to the present case. For simplicity we will assume all detectors having good efficiency ($\eta \gtrsim 0.9$) and $T \approx 1$. These assumptions allow us to simplify the resulting expression by neglecting terms of order higher than $(1-\eta)^2$. When we do that, instead of the $|\text{PS}\rangle$ we find the state $|\Psi_{\text{FE}}\rangle$ describing the field plus environment, the latter standing for losses coming from the nonunit efficiency detectors. We have,

$$\begin{aligned}
 |\Psi_{\text{FE}}\rangle \sim & (\sqrt{\eta}R)^N D(\alpha_{N+1})\hat{a}^\dagger T^{\hat{n}} D(\alpha_N)\hat{a}^\dagger T^{\hat{n}} \\
 & \times D(\alpha_{N-1}) \dots \hat{a}^\dagger T^{\hat{n}} D(\alpha_1)|0\rangle \hat{L}_0^\dagger \\
 & + R^{N-1} D(\alpha_{N+1})\hat{a}^\dagger T^{\hat{n}} D(\alpha_N)\hat{a}^\dagger T^{\hat{n}} \\
 & \times D(\alpha_{N-1}) \dots \hat{L}_1^\dagger T^{\hat{n}} D(\alpha_1)|0\rangle \times \\
 & \vdots \\
 & + R^{N-1} D(\alpha_{N+1})\hat{a}^\dagger T^{\hat{n}} D(\alpha_N)\hat{L}_{N-1}^\dagger T^{\hat{n}} \\
 & \times D(\alpha_{N-1}) \dots \hat{a}^\dagger T^{\hat{n}} D(\alpha_1)|0\rangle \\
 & + R^{N-1} D(\alpha_{N+1})\hat{L}_N^\dagger T^{\hat{n}} D(\alpha_N)\hat{a}^\dagger T^{\hat{n}} \\
 & \times D(\alpha_{N-1}) \dots \hat{a}^\dagger T^{\hat{n}} D(\alpha_1)|0\rangle, \tag{6}
 \end{aligned}$$

where, for brevity, we have omitted the kets corresponding to the environment. Here R is the reflectance of the beam splitter, $\hat{L}_0^\dagger = \mathbf{1}$ is the identity operator and \hat{L}_k , $k=1,2,\dots,N$, stand for losses in the first, second, ..., N th detector. Although the \hat{L}_k 's commute with any system operator, we have maintained the order above to keep clear the set of possibilities for photo absorption: the first term, which includes $\hat{L}_0^\dagger = \mathbf{1}$, indicates the probability for nonabsorption; the second term, which include \hat{L}_1^\dagger , indicates the probability for absorption in the first detector; and so on. Note that in case of absorption at the k th photodetector, the annihilation operator \hat{a} is replaced by the \hat{L}_k^\dagger creation Langevin operator. Other possibilities such as absorption in more than one detector lead to a probability of order lesser than $(1-\eta)^2$, which has been neglected.

Next, we have to compute the fidelity [24], $\mathcal{F} = \|\langle \Psi | \Psi_{\text{FE}} \rangle\|^2$, where $|\Psi\rangle$ is the ideal state given by Eq. (5) and $|\Psi_{\text{FE}}\rangle$ is the state given in the Eq. (6). The fidelity of PS versus parameter x is shown in the Fig. 3, for $N=5$ and three values of the photodetection efficiency. Note that the fidelity increases when the parameter x grows, showing that high values of fidelity occur when the PS resembles the vacuum state. It also shows that fidelity increases when efficiency η grows, as it should.

The foregoing results show that losses caused by the presence of non-ideal photodetectors will transform our desired pure PS in a mixed state. As consequence, employing a modified state to measure a certain property one will end up with

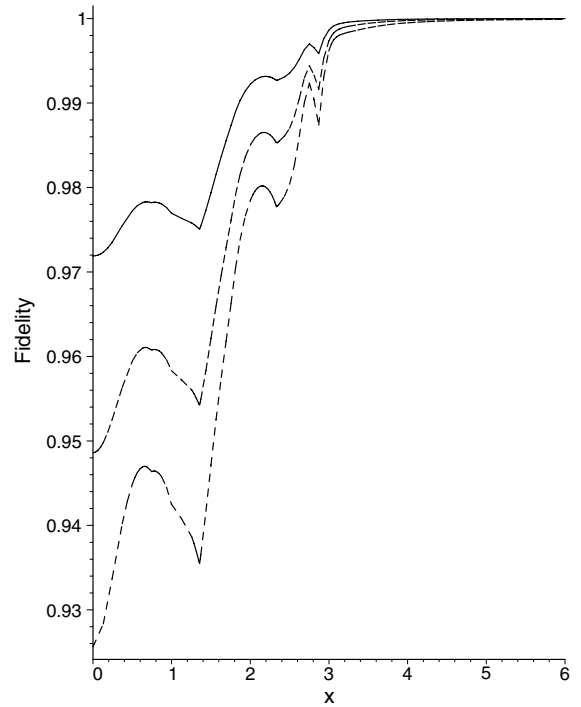


Fig. 3. Plot of fidelity versus x for $N=5$ and the photodetector efficiencies $\eta=0.90$ (dotted), $\eta=0.95$ (dashed) and $\eta=0.98$ (solid).

a modified property. So, a pertinent question is how to circumvent this difficulty. Fortunately, there is a solution to this problem provided by the inverse Bernoulli convolution (IBC), allowing one to reconstruct the desired pure state from the mixed state. Such procedure has been implemented in distinct scenarios [25,26]. In this procedure a pure state, represented by the density operator $\hat{\rho}_p = |\Psi\rangle\langle\Psi|$, can be reobtained from the smeared data contained in the mixed density operator. From these data contained in the density operator $\rho_{\text{out}}(\mathbf{k},\boldsymbol{\eta})$ one recovers the pure state $\hat{\rho}_p$ as [26]:

$$\begin{aligned}
 \hat{\rho}_p = & \frac{1}{P_0(\mathbf{1})} \sum_{k_1, \dots, k_n} \{b_{o;k_1}(\eta_1^{-1}) \dots b_{o;k_N}(\eta_N^{-1}) \\
 & \times P_{\mathbf{k}}(\boldsymbol{\eta})\rho_{\text{out}}(\mathbf{k}, \boldsymbol{\eta})\}, \tag{7}
 \end{aligned}$$

where the functions $b_{o;ki}$ are defined by

$$b_{l,m}(z) = \binom{m}{l} z^l (1-z)^{m-l} \tag{8}$$

and $\mathbf{k}=(k_1,\dots,k_N)$, $\boldsymbol{\eta}=(\eta_1,\dots,\eta_N)$, with k_j being the number of counts obtained in the detectors D_j with efficiency η_j . Here $p_{\mathbf{k}}(\boldsymbol{\eta})$ stands for the probability of this composite event. The IBC is relevant when the fidelity of the wanted state is not enough for a certain purpose. The reconstruction given in the Eq. (7) can be applied to whatever statistics of interest [26]. Now, a question emerging concerns the number of data required for the IBC. As explained in [25] one needs to construct the photocount distribution in the detectors D_j . Let N' be the total number of measurements (each one involving all detectors) and X_n the number of those corresponding to n photons ($n=0,1,2,\dots,M$); M is a cutoff parameter for large photon number.

The choice on N' leads to a statistical error (SE) in the photocounting scheme. For a given cutoff M there exists a minimal N'_ϵ for every small ϵ that if $N' > N'_\epsilon$ then the SE is smaller than ϵ . So, the cutoff reduces the SE by increasing the number of measurements. In resume, the required number of data depends on the desired accuracy for each specific target (see, e.g., Eq. (20) of [25]). The method is somewhat slow-going, but it does not waste any trials [25,26].

At this point the following enlightening explanation is opportune: the IBC is no more than a theoretical correction, hence not able to experimentally purify the mixing caused by non-ideal detectors. The reconstruction is made upon

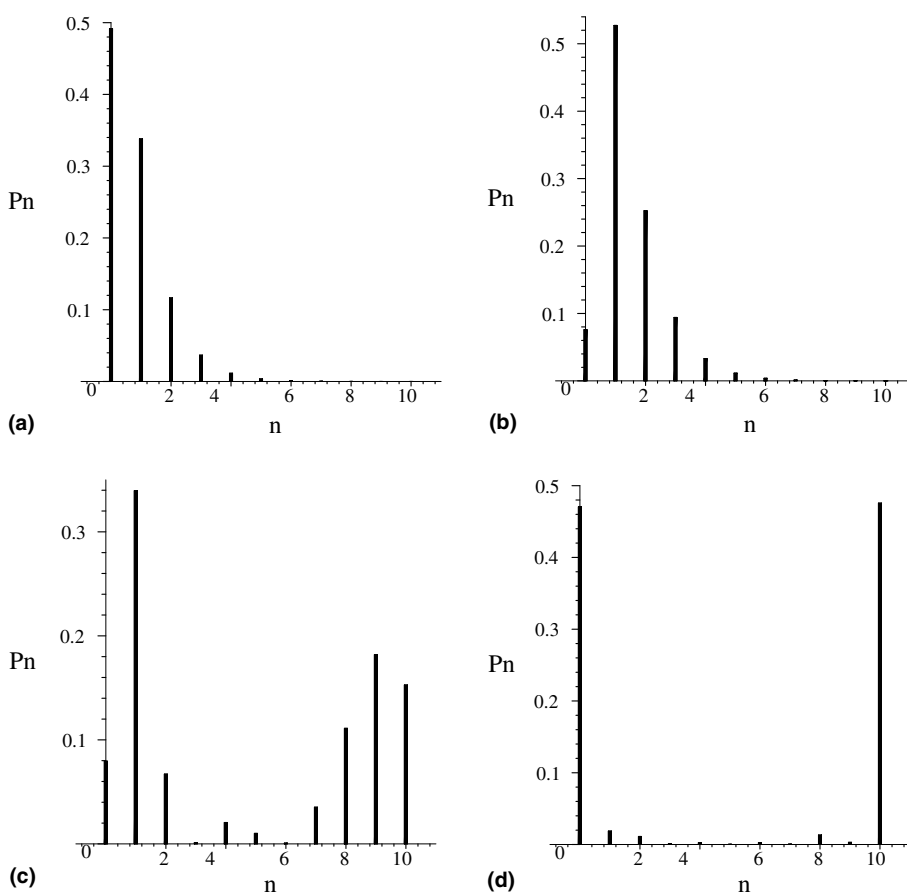


Fig. 4. Plots of the photon-number distribution P_n versus n , for the PS, with $N=10$ and $x=5.02$ (a), 4.90 (b), 2.44 (c) and 0.18 (d).

computer data, not being an action upon the running field states themselves. However, when applying the modified (smeared) output state in the measurement of certain property of another field state one finally ends up with some measurement data (a set of numbers inside a computer and not a quantum state) these numbers being the final outcome of the entire procedure. Reconstruction of the initial data (the auxiliary pure state) yields the reconstruction of the final data (the measured property of another field state). So, it does not matter how this property has been obtained, whether theoretically or not. It is also pertinent mentioning that the IBC will no longer be used when technological advances achieve photodetectors with efficiency near 100%.

3. Statistical properties of the PS

3.1. Photon number distribution

From Eq. (1) defining the PS we find the statistical distribution $P_n = |C_n|^2$, where the C_n are the coefficients appearing in the expansion of the PS in the Fock's basis: $|PS\rangle = \sum_{n=0}^N C_n |n\rangle$. In this way we obtain,

$$P_n = \mathcal{N}^2 \binom{N}{n}^{-1} \frac{H_{N-n}^2(x/\sqrt{2})}{[2(N-n)-1]!!}. \quad (9)$$

Fig. 4 shows the statistical distribution, P_n versus n , for various values of the parameter x . We note that, for certain choices of parameters, the statistical distribution of the PS resembles that of the thermal state with $\langle \hat{n} \rangle = 0.76$ (Fig. 4(a), for $x=5.02$); that of a coherent state $|\alpha\rangle$ with $\alpha=1.3$ (Fig. 4(b), for $x=4.90$) and that exhibiting oscillations (Fig. 4(c), for $x=2.44$) an effect connected with interference in the phase space [27]. ‘Exotic’ distributions are also displayed by the PS, as one in which $P_n = 0.5(\delta_{n,0} + \delta_{n,N})$, where only the lowest and highest states partake the statistical distribution (see Fig. 4(d) for $x=0.18$). Another interesting feature appears for $x=0$ when the statistical distribution exhibits parity, being either even or odd according to the parity of the Hilbert space dimension N (not shown in figures).

3.2. Sub-Poissonian statistics

Sub-Poissonian (SP) effect is usually studied via the Mandel Q -parameter [28],

$$Q = (\Delta \hat{n}^2 - \langle \hat{n} \rangle^2) / \langle \hat{n} \rangle, \quad (10)$$

where $\Delta \hat{n}^2 = \langle \hat{n}^2 \rangle - \langle \hat{n} \rangle^2$, with $\langle \hat{n}^k \rangle = \langle PS | \hat{n}^k | PS \rangle$, $k=1,2$. The SP effect results when $Q < 0$, namely: $\Delta \hat{n}^2 < \langle \hat{n} \rangle$.

The substitution of Eq. (1) in the Eq. (10) furnishes the value of the Mandel Q -parameter for the PS. Fig. 5 exhibits plots of the Mandel Q -parameter as function of x , for $N=2,3,5$.

Note that the x -interval for which the PS exhibits SP-effect decreases when the dimension N of the Hilbert space grows. The effect itself diminishes for growing N and, for large values of x , the PS no longer exhibits the SP-effect. We have observed that for large values of N ($N > 20$) the SP-effect of the PS disappears.

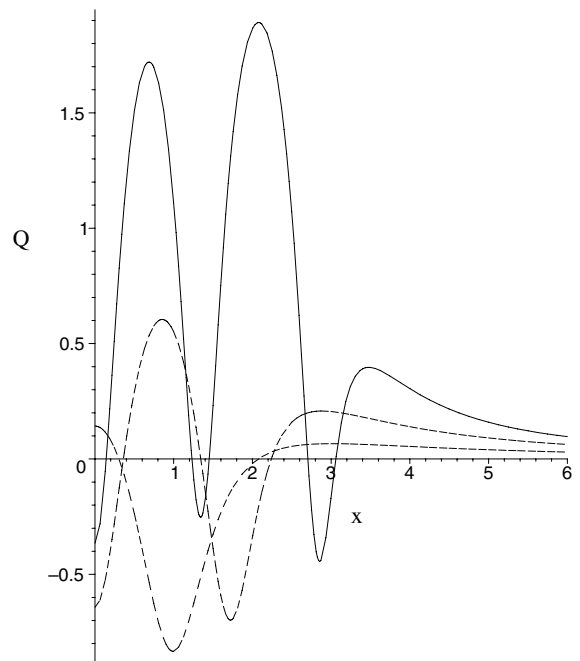


Fig. 5. Plot of the Mandel Q -parameter for the PS as a function of x for $N=2$ (pointed curve), $N=3$ (solid curve), and $N=5$ (dotted curve).

4. Comments and conclusion

In this brief report, we have studied the generation of the PS, required in the scheme introduced in [18] to measure variances of quadrature operators – as shown in [19]. Since the scheme in [18] deals with travelling fields, we have used a method in [5], appropriated for this scenario. The ideal case, where the components of the apparatus (mirrors, beam-splitters, photodetectors) are assumed excellent, was considered and the success probability was calculated as a function of x (Fig. 2). We have also discussed the influences of non-ideal components upon the fidelity \mathcal{F} of the state. For typical values available by the recent technology we have taken ideal beam-splitters and photodetectors having efficiencies $\eta=90\%$ corresponding results exhibited in Fig. 3 [29].

It is worth mentioning that the success probability of a generation-method depends on the desired state being prepared. This explain why the present success is greater than that obtained for the state exemplified in [5]. This comparison shows that, given a desired state to be prepared and various available generation-methods, the question about which of them is the best will be answered only after a comparison case by case.

For completeness we have also studied some interesting statistical features of the PS, such as photon number distribution and sub-Poissonian statistics (Section 3, Figs. 4 and 5).

Acknowledgement

We are indebted to Dr. J. Clausen for enlightening discussions concerning the inverse Bernoulli convolution. We thank the CNPq, Brazilian Agency, for partially supporting this work.

References

- [1] K. Vogel, V.M. Akulin, W.P. Schleich, Phys. Rev. Lett. 71 (1993) 1816;
- A.S. Parkins, et al., Phys. Rev. Lett. 71 (1996) 3095;
- C.K. Law, J.H. Eberly, Phys. Rev. Lett. 76 (1996) 1055;
- B.M. Garraway, et al., Phys. Rev. A 49 (1994) 535.
- [2] M. Brune, et al., Phys. Rev. Lett. 65 (1990) 976;
- Phys. Rev. A 45 (1992) 5193;
- M. Brune, et al., Phys. Rev. Lett. 72 (1994) 3339;
- L. Davidovich, et al., Phys. Rev. A 50 (1994) R895;
- S.B. Zeng, G.C. Guo, Phys. Lett. A 244 (1998) 512.
- [3] D.T. Pegg, L.S. Phillips, S.M. Barnett, Phys. Rev. Lett. 81 (1998) 1604;
- S.A. Babichev, J. Ries, A.I. Lvovsky, Europhys. Lett. 64 (2003) 1.
- [4] O. Steuernagel, Opt. Commun. 138 (1997) 71;
- M. Paris, Phys. Rev. A 62 (2000) 033813.
- [5] M. Dakna, et al., Phys. Rev. A 59 (1999) 1658;
- Phys. Rev. A 60 (1999) 726.
- [6] C.C. Gerry, Phys. Rev. A 59 (1999) 4095;
- G.M. D'Ariano, et al., Phys. Rev. A 61 (2000) 053817.
- [7] Y.A. Guimarães, et al., Phys. Lett. A 268 (2000) 260;
- C.J. Villas-Boas, et al., Phys. Rev. A 63 (2001) 55801.
- [8] C.J. Villas-Boas, N.G. de Almeida, M.H.Y. Moussa, Phys. Rev. A 60 (1999) 2759.
- [9] D.M. Meekhof, et al., Phys. Rev. Lett. 76 (1996) 1796;
- Science 272 (1996) 1131;
- J.I. Cirac, et al., Adv. At. Mold. Opt. Phys. 37 (1996) 237;
- D.J. Wineland, et al., J. Res. Natl. Inst. Stand. Technol. 103 (1998) 259.
- [10] A.L. Souza, et al., Phys. Lett. A 208 (2001) 235.
- [11] C.H. Bennett, et al., Phys. Rev. Lett. 70 (1993) 1895;
- D. Bowmester, et al., Nature 390 (1997) 575;
- B. Julsgaard, et al., Nature 413 (2001) 400.
- [12] B.E. Kane, et al., Nature 393 (1998) 143;
- P.L. Knight, W.J. Munro, Quantum Computer, Quantum Criptografy and Teleportation (Encyclopedia of Optical and Engineering, DO 10.10811/E-EQE 120009560 (2003).
- [13] T. Pellizzari, Phys. Rev. Lett. 79 (1997) 5242;
- I. Abram, P. Grangier, C.R. Physique 4 (2003) 187;
- G.A. Barbosa, Phys. Rev. Lett. 90 (2003) 227901.
- [14] N. Gisin, et al., Rev. Mod. Phys. 74 (2002) 145.
- [15] See, e.g., G. Björk, L.L. Sanchez-Soto, Phys. Rev. Lett. 86 (2001) 4516;
- M. Mützel, et al., Phys. Rev. Lett. 88 (2002) 083601 and references therein.
- [16] W.H. Zurek, Phys. Today 44 (1991) 36;
- C.C. Gerry, P.L. Knight, Am. J. Phys. 65 (1997) 964;
- B.T.H. Varcoe, et al., Nature 403 (2000) 743;
- G.S. Agarwal, M.O. Scully, H. Walther, Phys. Rev. Lett. 86 (2001) 4271.
- [17] B. Yurke, D. Stoler, Phys. Rev. Lett. 57 (1986) 13.
- [18] S.M. Barnett, D.T. Pegg, Phys. Rev. Lett. 76 (1996) 4148.
- [19] B. Baseia, M.H.Y. Moussa, V.S. Bagnato, Phys. Lett. A 231 (1997) 331.
- [20] C. Valverde, et al., Phys. Lett. A 315 (2003) 213.
- [21] A.T. Avelar, N.G. de Gomes, B. Baseia, J. Opt. B: Quantum Semiclass. Opt. 5 (2004) 1.
- [22] O. Steuernagel, J.A. Vaccaro, Phys. Rev. Lett. 75 (1995) 3201.

- [23] Recent technological advances yield photodetector efficiency about 95%. See e.g. P.G. Kwiat, et al., Phys. Rev. A 48 (1993) R867;
J. Kim, et al., Appl. Phys. Lett. 74 (1999) 902;
S. Takeuchi, et al., Appl. Phys. Lett. 74 (1999) 1063;
D.F.V. James, P.G. Kwiat, Phys. Rev. Lett. (2002) 183601.
- [24] The expression $\mathcal{F} = |\langle PS | \Psi_{FE} \rangle|^2$ stands for usual abbreviation in literature. Actually, this is equivalent to $\langle PS | Tr_E \hat{\rho}_{FE} | PS \rangle$, where $\hat{\rho}_{FE} = |\Psi_{FE}\rangle\langle\Psi_{FE}|$ and $Tr_E \hat{\rho}_{FE}$ is the smeared (mixed) state, mentioned before.
- [25] T. Kiss, U. Herzog, U. Leonhardt, Phys. Rev. A 52 (1995) 2433.
- [26] M. Dakna, et al., Acta Phys. Slov. 48 (1998) 207.
- [27] W. Schleich, J.A. Wheeler, Nature 326 (1987) 574.
- [28] L. Mandel, Opt. Lett. 4 (1979) 205;
R. Short, L. Mandel, Phys. Rev. Lett. 51 (1983) 384;
S. Brattke, et al., Phys. Rev. Lett. 86 (2001) 3535;
L. Davidovich, Rev. Mod. Phys. 68 (1996) 127.
- [29] Although the use of ideal detectors improves the fidelity of the prepared states, the generation of nonclassical states with inefficient detectors is highly topical, as exemplified in: A.P. Lund, et al., quantum-ph/0401001.